

Measurements of radiation levels inside the ESRF storage ring

*P. Berkvens & P. Colomp
European Synchrotron Radiation Facility*

Abstract

Radiation damage observed on a number of cables in the storage ring has triggered a series of radiation measurements inside the storage ring to assess dose levels during injection and during stored beam conditions. Photon dose rates have been measured in different locations, using small ionization chambers. The results show a strong spatial variation of the measured dose rates and indicate that the radiation damage is essentially due to synchrotron radiation. The measured dose levels allow us to make estimations of the integrated dose in certain areas of the storage ring over the lifetime of the ESRF. The paper also describes a beam loss monitoring system, using 32 ionization chambers installed inside the storage ring, allowing the quantifying of beam losses.

1. Introduction

Radiation damage has been observed on a number of accelerator components in the ESRF storage ring. In particular, damage occurring on cables becomes worrying. Although it is obvious that the damage on cables is essentially caused by electromagnetic radiation, it is not clear whether the origin is synchrotron radiation or bremsstrahlung. A number of radiation measurements inside the storage ring to assess dose levels during injection and during stored beam conditions have therefore been made, in order to determine the origin of the radiation damage. From the results of these measurements estimations can be made concerning values for the expected integrated dose, which is an important information when replacing damaged cables.

In order to interpret the importance of the bremsstrahlung component in the measured radiation levels, we need to quantify local beam losses. The following section therefore describes one type of beam loss monitors installed inside the ESRF storage ring, and shows how we can obtain absolute values for beam losses from these monitors.

2. Estimation of local beam loss distributions

Inside the storage ring tunnel 32 PTW 50 litre ionisation chambers are installed, one per unit cell. As schematically shown in figure 1, these monitors are placed on the floor, next to the first dipole of the achromat. They are read out using PTW Unidos electrometers, in integrating mode. These ionisation chambers are placed inside a 1 cm thick lead shield. This lead shielding sufficiently attenuates the synchrotron radiation so that these monitors measure essentially bremsstrahlung radiation. These ionisation chambers are calibrated at PTW-Freiburg and since they are all installed at an identical location within each unit cell, it will be possible to use these monitors as beam loss monitors. This is illustrated hereafter.

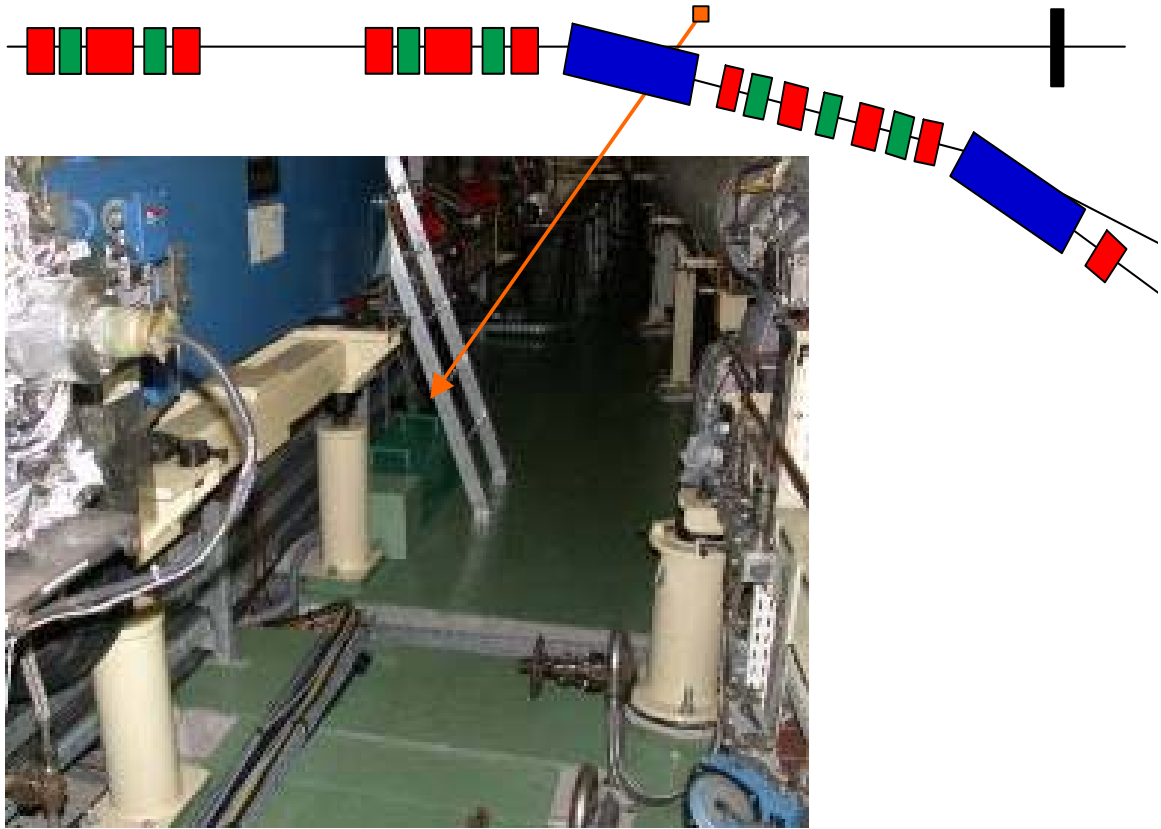


Figure 1: Picture of one of the 32 beam loss monitors, showing schematically their location within each unit cell.

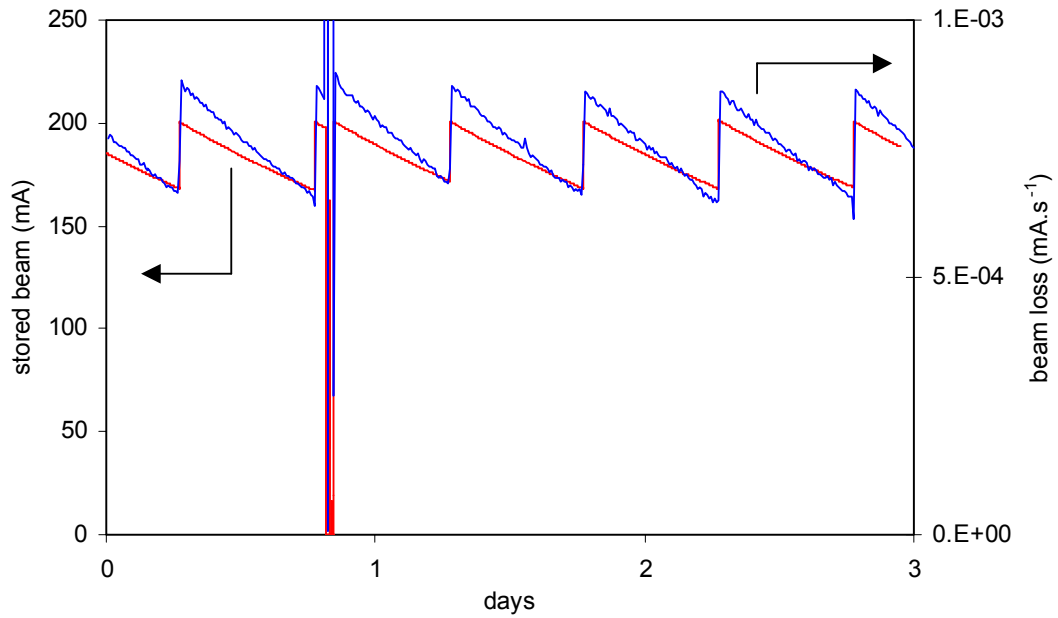


Figure 2: Stored beam profile (red) and corresponding total beam losses (blue) for three days of uniform fill operation.

Figure 2 shows the stored beam pattern during three days of uniform filling operation. The corresponding total beam loss rate is also shown. Figure 3 shows the readings from the 32 undulos beam loss monitors during these 3 days of uniform filling. One sees that the beam losses occur essentially in a relative small number of cells. Cell 4 contains the injection septa as well as a pair of horizontal scrapers. This explains the high losses in this cell. Cell 6, apart from containing one of the 8 mm ID vacuum vessels, sees a lot of the losses occurring on the vertical scrapers installed at the end of cell 5. Finally one sees quite dramatic changes on the beam loss monitors of cells 9 and 13. These cells are equipped with in-vacuum undulators, and the changes correspond to changes of the gaps of these in-vacuum undulators. One notes that these gap changes also induce variations elsewhere, essentially on the beam loss monitors of cells 4 and 6.

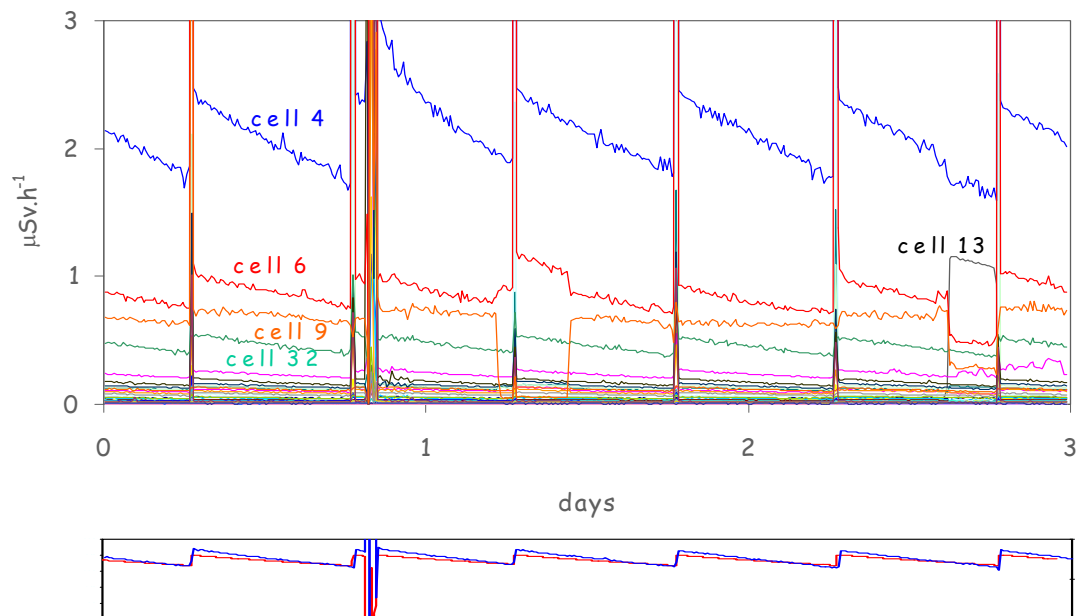


Figure 3: Readings from the 32 beam loss monitors during the 3 days of uniform filling of figure 2.

We can now reconstruct the total beam losses shown in figure 2 from the readings of the individual beam loss monitors, by making a weighted sum. Figure 4 shows the total beam loss obtained with the following expression

$$BL_{\text{total}} = \sum_{i=1,32} a_i \times BL_i, \text{ with } a_i = 1, \text{ for } i \neq 6$$

$$a_i = 2.6, \text{ for } i = 6$$

where BL_i corresponds to the reading of the i th beam loss monitor. The value of 2.6 for a_6 is chosen such that the step variations from the changes in the gaps of the in-vacuum undulators disappear from the total beam loss profile. We can easily explain the fact that we have to multiply the reading of the cell 6 beam loss monitor by a value higher than one by the fact that this monitor sees also the losses from the scraper at the end of cell 5, but in a more attenuated way because of the larger

distance. One notices a significant higher beam loss value obtained from the beam loss monitors at the beginning of the beam decay after the beam loss. This artefact is explained from the induced activation caused by the large electron charge injected during the few unsuccessful injections after the beam loss. This decaying induced activity, essentially around the scrapers and the injection septum is clearly measured with the monitors in cells 4 and 6.

With this formalism we obtain a calibration factor of $1.1 \cdot 10^{-4} \text{ mA}\cdot\text{s}^{-1} \times (\mu\text{Sv}\cdot\text{h}^{-1})^{-1}$ to derive absolute beam losses from the beam loss monitor readings. The validity of this formalism has been verified by applying the same calibration factor to other filling patterns, with substantially different loss rates.

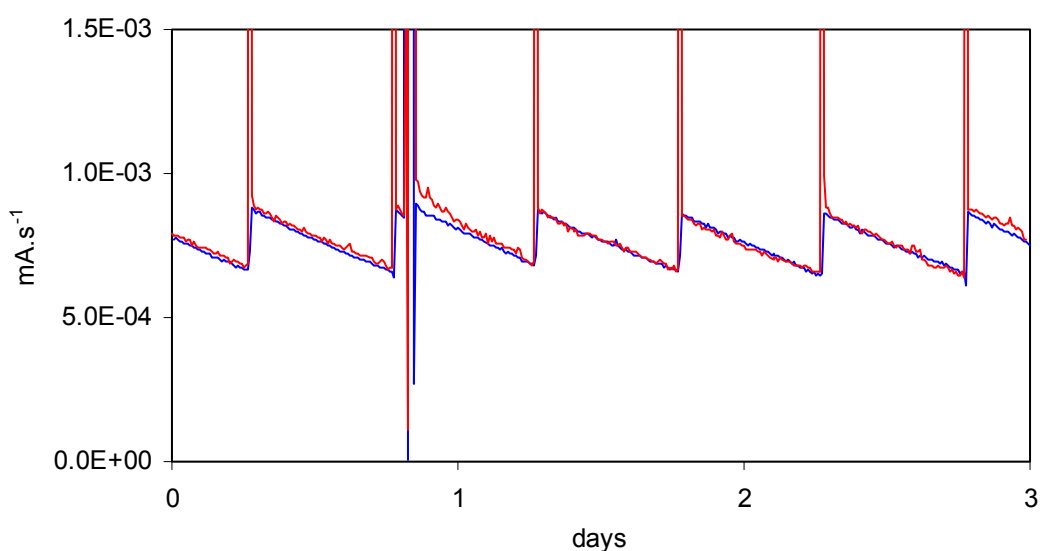


Figure 4: Comparison between total beam losses obtained from beam decay (blue) and obtained from the unidos beam loss monitors (red).

We can also look at the relative beam losses in each cell. Figure 5 shows a typical example taken during one of the beam decays of figure 2. We see that a large number of cells see losses less than 1 % of the total losses.

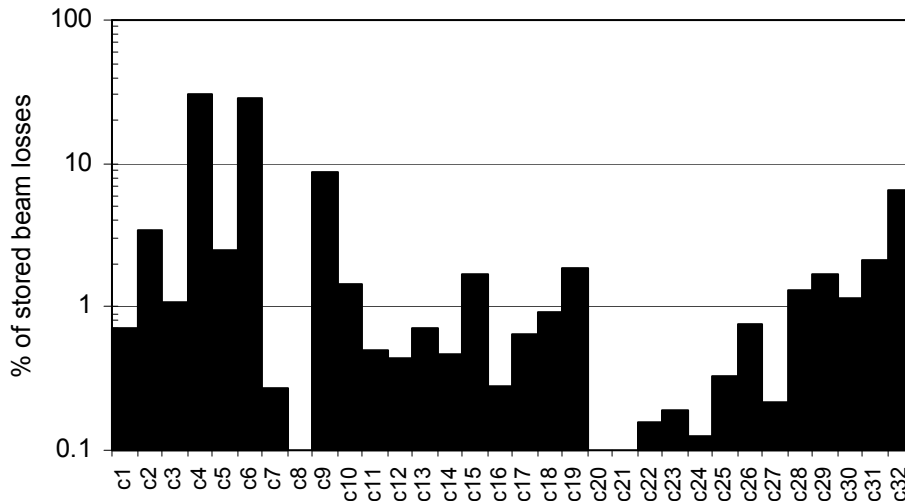


Figure 5: Typical relative beam loss distribution throughout the storage ring.

3. Radiation measurements inside the storage ring

Radiation damage inside the ESRF storage ring has become a serious problem. Damage on a number of cables are particularly worrying. We have therefore carried out a series of radiation measurements to determine the origin of the problem (synchrotron radiation or bremsstrahlung) and to quantify dose levels. In the case of radiation damage to cables we do not expect the problem to come from neutrons because of their relatively low dose. Other types of radiation damage, e.g. demagnetisation of permanent magnets could however be caused essentially by neutrons.

We used small 0.6 cm^3 ionisation chambers, measuring air kerma, which were placed at various locations inside the storage ring in cell 6, and recorded the dose rates during injection and during stored beam conditions. Using the beam loss monitors as explained above we could quantify the local beam losses inside cell 6 (+ scrapers end of cell 5) during our measurements. Figure 6 shows the relative beam losses obtained from the unidos beam loss monitors during the various fills and decays. We see that during injection we had typically 20 % of the total losses in cell 6 (+ scrapers cell 5) whereas these local losses vary during beam decay typically between 40 % and 60 %. The overall injection efficiency was around 75 %. From the previous section - see figure 5 - we know that the local losses in the majority of the 32 individual storage ring cells are much smaller than the values quoted here. Therefore bremsstrahlung dose levels measured here will be significantly higher than what should be expected in most cells.

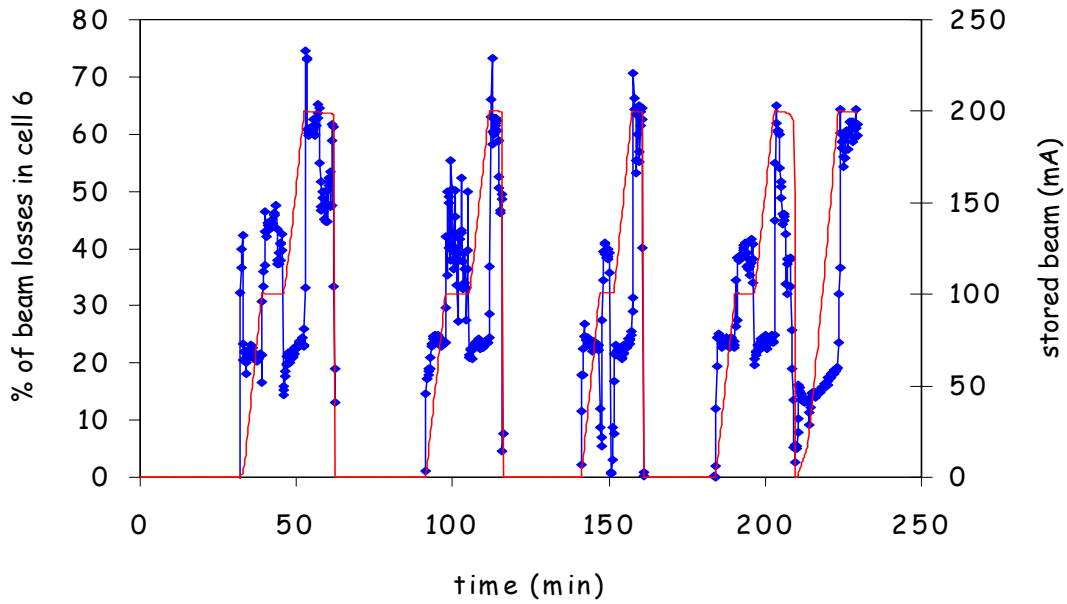


Figure 6: Relative beam losses in cell 6 during the different fills and beam decays (blue). The stored beam profile is shown in red.

Figure 7 and table 1 indicate the different locations where radiation measurements were done. The third column of table 1 indicates whether for the given location the measured dose levels were due to synchrotron radiation or were due to bremsstrahlung. Figure 8 shows a typical measurement in a location where the dose is due to synchrotron radiation. One sees that, both during injection and during stored beam, dose rates are indeed proportional to stored beam intensity. We see from table 1 that this situation occurred during the first six measurements. In location 7 the radiation was however completely determined by bremsstrahlung. This is shown in figure 9, where one sees a more or less constant dose level during injection, caused by the injection losses, with much smaller dose rates during stored beam, due to the much smaller stored beam losses as compared to the injection losses. One also notices the increased dose rates during the beam dump at the end of the measurement.

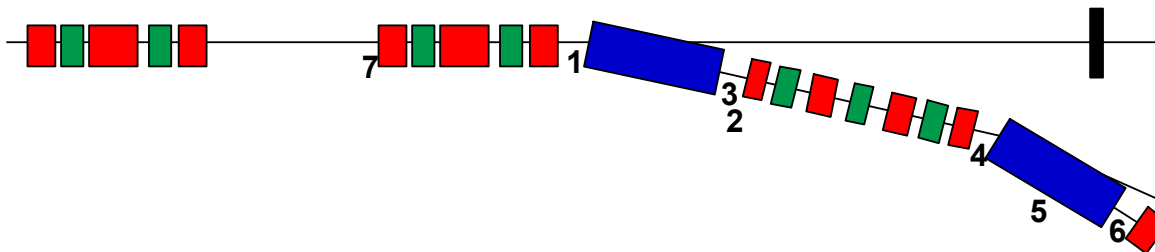


Figure 7: Locations of different radiation measurements.

| position | description | type of radiation |
|----------|---|-----------------------|
| 1 | entrance of dipole, beam height | synchrotron radiation |
| 2 | exit of dipole, crotch vessel, penning gauge cable, beam height | synchrotron radiation |
| 3 | exit of dipole, end flange of vacuum vessel, beam height | synchrotron radiation |
| 4 | entrance of dipole, bellows, beam height | synchrotron radiation |
| 5 | middle of dipole, beam height | synchrotron radiation |
| 6 | exit of dipole, end flange of vacuum vessel, beam height | synchrotron radiation |
| 7 | exit of ID vessel, above beam axis | bremsstrahlung |

Table 1: Description of the different measurement locations.

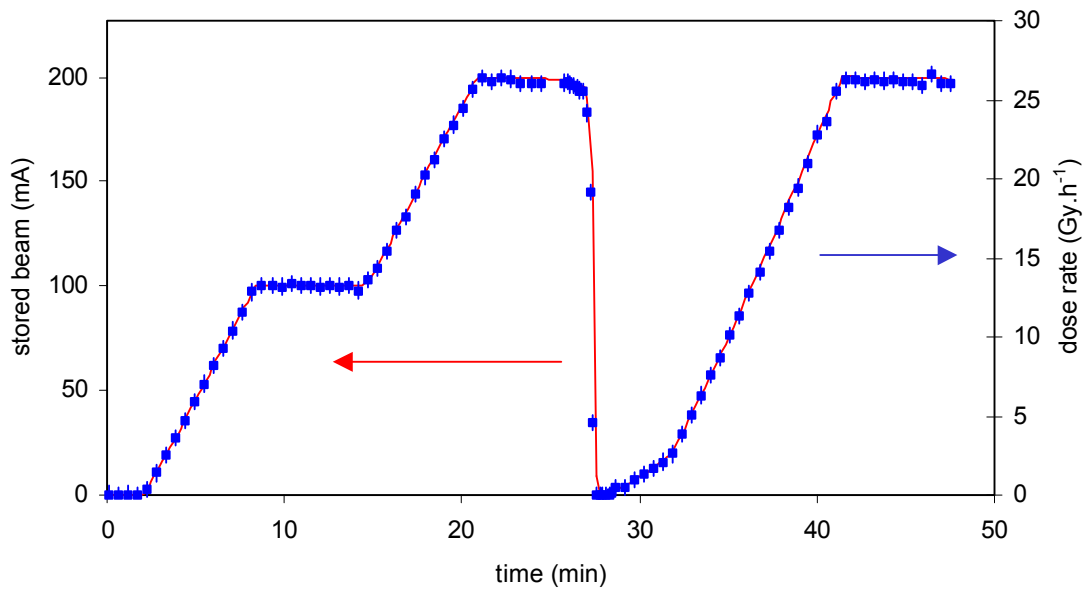


Figure 8: Dose rate pattern measured in location 6, footprint of a synchrotron radiation dominated field.

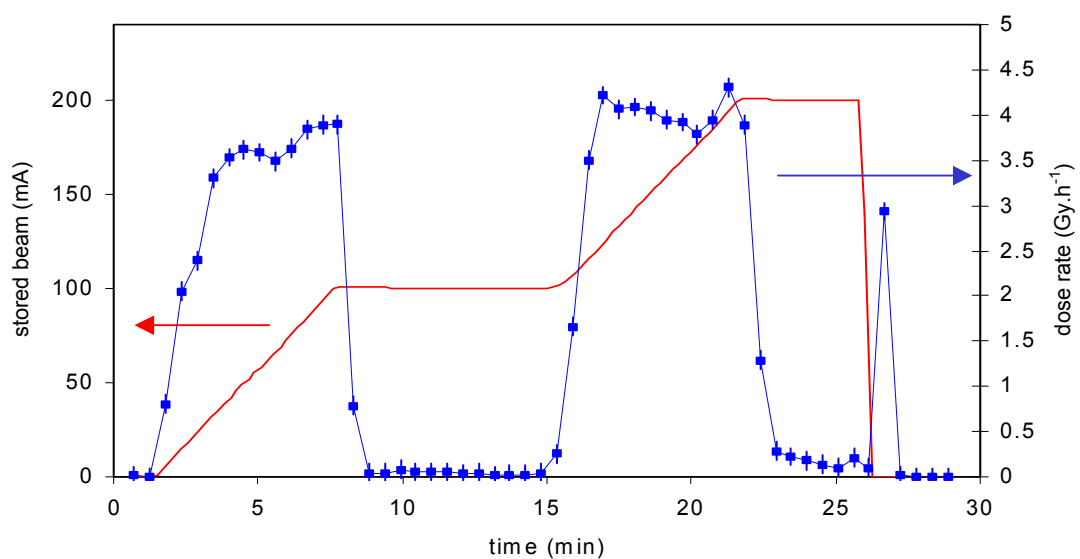


Figure 9: Dose rate pattern measured in location 7, showing a bremsstrahlung dominated radiation field.

Table 2 shows the measured synchrotron radiation dose rates for locations 1 to 6, corresponding to a 200 mA stored beam. One notices the large variation by more than two orders of magnitude in the measured dose rates. The highest values, measured at the end of the dipoles, are explained by scattered radiation from the crotch absorbers. The most severe problems of radiation-damaged cables were indeed recorded in these areas.

| Location | Measured dose rate (Gy.h ⁻¹) for a 200 mA stored beam |
|----------|--|
| 1 | 0.15 |
| 2 | 3.7 |
| 3 | 15.8 |
| 4 | 1.4 |
| 5 | 0.15 |
| 6 | 26.5 |

Table 2: Measured dose rates for locations 1 to 6, for a stored beam of 200 mA.

4. Discussion

The results in table 2 show that the highest dose levels occur in the areas close to the crotch vessels, where the majority of the dipole synchrotron radiation is absorbed. These are typically the areas where the most severe radiation damage occurs, in particular to cables. From the measured dose rates, we will estimate values for the total dose that will be integrated after e.g one year of operation. A good estimation of these integrated doses are essential information when replacing damaged cables, to choose cables as a function of their radiation resistance, and to decide whether radiation shields should be foreseen.

Figure 10 shows the stored beam pattern recorded during two months of operation during June and July of 2002. The integrated electron dose (A.h) is also shown on the figure. In the case of a synchrotron radiation determined field, the integrated radiation dose will be proportional to this integrated electron dose. We see that a typical week of multi-bunch operation will integrate an electron dose around 27 A.h. The integrated dose during 16-bunch mode, and even more single bunch operation, will of course be much smaller. Taking into account the operation cycles of the ESRF, and the distribution between the different filling patterns, we integrate typically 900 A h during one calendar year. Using this value and the measured dose rates from table 2, we obtain the estimated values for the integrated radiation dose for one year of operation for the positions 1 to 6, shown in table 3.

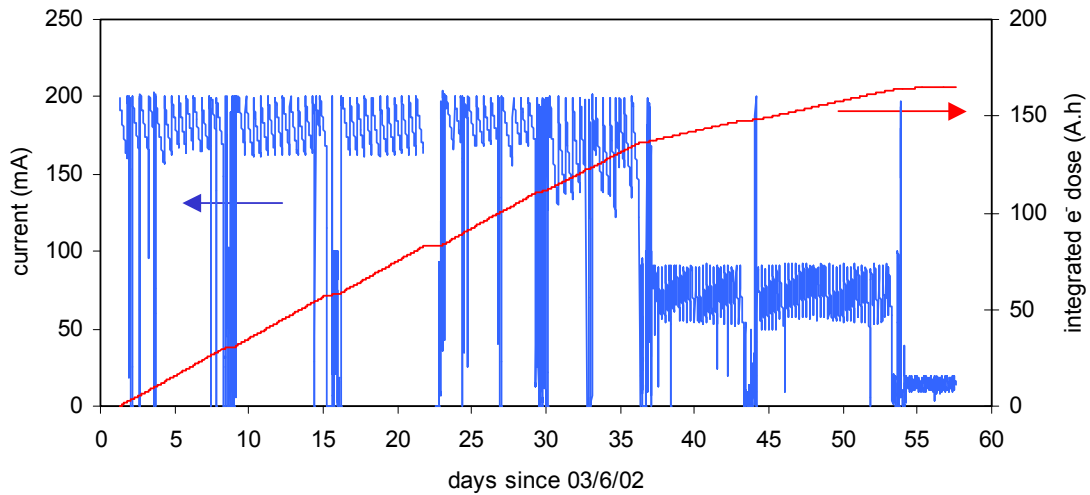


Figure 10: Typical stored beam pattern (blue), and corresponding integrated electron dose (red).

| Location | Estimated integrated dose (Gy.y^{-1}) after one year of nominal operation |
|----------|---|
| 1 | 675 |
| 2 | $1.7 \cdot 10^4$ |
| 3 | $7.1 \cdot 10^4$ |
| 4 | 6300 |
| 5 | 675 |
| 6 | $1.2 \cdot 10^5$ |

Table 3: Estimated annual integrated doses for locations 1 to 6.

The measured values around the crotch vessels were confirmed by another series of measurements, carried out at the exit of the 1st dipole of cell 11. Figure 11 shows the location of the 5 measurements carried out, with the corresponding values given in table 4. As can be seen, the measured dose rates vary by almost a factor of 10 over a few cm.

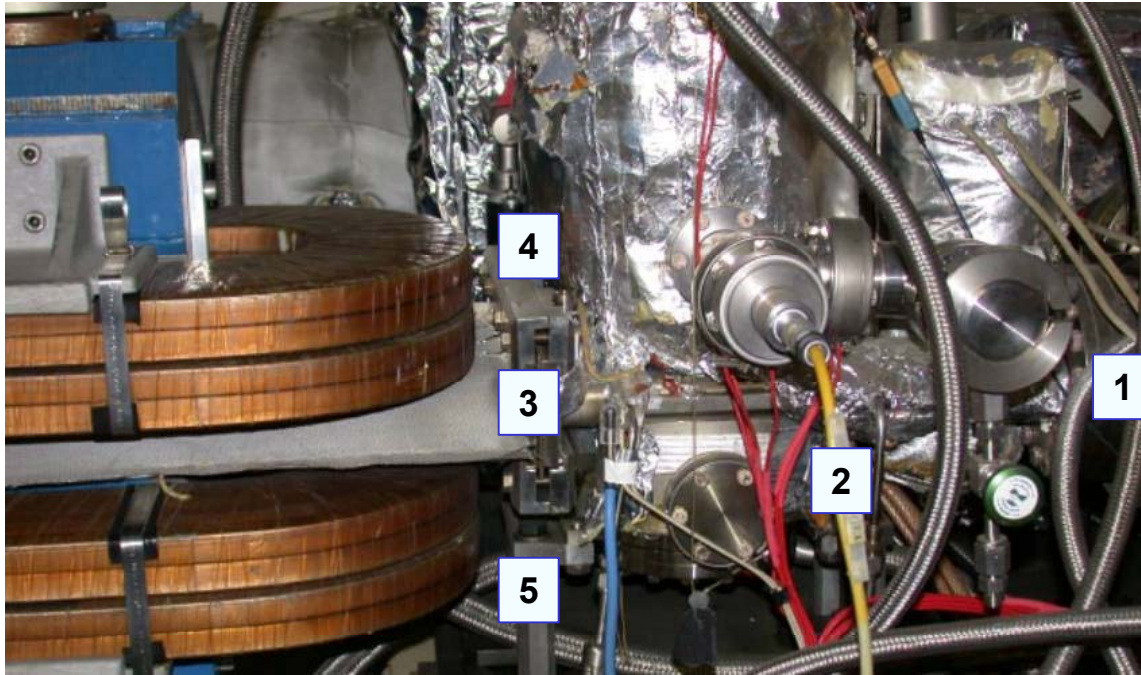


Figure 11: Positions of the 5 measurements carried out in cell 11.

| Location | Measured dose rate ($\text{Gy}\cdot\text{h}^{-1}$) for a 200 mA stored beam | Estimated integrated dose ($\text{Gy}\cdot\text{y}^{-1}$) after one year of nominal operation |
|----------|--|---|
| 1 | 3.8 | $1.7 \cdot 10^4$ |
| 2 | 5.2 | $2.3 \cdot 10^4$ |
| 3 | 28.0 | $1.3 \cdot 10^5$ |
| 4 | 6.4 | $2.9 \cdot 10^4$ |
| 5 | 7.8 | $3.5 \cdot 10^4$ |

Table 4: Measured dose rates and estimated annual integrated doses for locations 1 to 5 in cell 11.

In reference [1] it was shown that the injected charge in the storage per year roughly corresponds to 1800 injections from 0 to 200 mA. From figure 9 we see that in position 7 a total dose of 0.9 Gy is integrated per 200 mA injection. We can therefore estimate the total integrated dose per calendar year for position 7 as 1620 Gy. As explained above, this value should largely overestimate the bremsstrahlung dose rates in most of the storage ring cells. Radiation damage from bremsstrahlung should therefore be rather limited compared to synchrotron radiation induced damage.

Reference

- [1] P. Berkvens and P. Colomp, Estimation of radioactivity inventory of the ESRF, these proceedings